

Study of color connections in e^+e^- annihilation

Feng-lan Shao¹, Q u-bing X ie^{2,†,‡}, Shi-yuan Li¹, and Q un W ang¹

¹Physics Department, Shandong University,

Jinan, Shandong 250100, P.R. China and

²China Center of Advanced Science and Technology (CCAST), Beijing 100080, P.R. China

(Dated: March 10, 2022)

Abstract

We replace in the event generator JETSET the color singlet chain connection with the color separate state one as the interface between the hard and soft sectors of hadronic processes. The modified generator is applied to produce the hadronic events in e^+e^- annihilation. It describes the experimental data at the same level as the original JETSET with default parameters. This should be understood as a demonstration that color singlet chain is not the unique color connection. We also search for the difference in special sets of three-jet events arising from different color connections, which could subject to further experimental test.

PACS numbers: 13.87.Fh, 12.38.Bx, 12.40.-y, 13.66.Bc

Electronic address: shao @ mail.sdu.edu.cn

[‡]Electronic address: xie@ sdu.edu.cn

I. INTRODUCTION

Strong interaction processes in high-energy reactions, e.g. $e^+e^- \rightarrow$ hadrons, are generally described by two distinct sectors: the perturbative and hadronization phases. The perturbative phase is well described by perturbative quantum chromodynamics (PQCD), while the hadronization one is non-perturbative and currently can only be described by hadronization models [1][2]. A natural problem arises as how to link these two phases, which is beyond the capability of PQCD. In present hadronic event generators [3][4], the color connections are assumed to be the color string or the color cluster chain. This is true only in the case of $N_c \rightarrow \infty$, because with infinitely many colors the probability that two or more partons have accidentally the same color is zero, and then the way to connect the partons by a string or a cluster chain becomes unique [5][6]. The present hadronization models work quite well, which shows that the large N_c limit does reflect some features of the real world. However, with only three colors in nature, the color structure of a multiparton state at the end of the parton cascade is copious and complex [6] – [9]. The one that is used in the current string and cluster models is called the color singlet chain (CC) state, where in each string piece or cluster the color charge from one parton is connected to its anti-color from the other, so that the string piece or the cluster is color neutral. This results in a color neutral flow in the string or the cluster system [8][9]. PQCD calculation shows that, when projected onto the color space of the multipartonic state, the CC state occurs with a probability less than 1 and the probability decreases as the growing number of partons [8][10]. Part of the rest probability goes to such states as the so called color separate (CS) singlet, where a multiparton system separates itself into several color singlet subsystems and each subsystem can hadronize independently [5][6] [11][12].

The presence of CS states can be easily understood in $e^+e^- \rightarrow qq + n\text{gluons} + h^0$'s process. If two gluons have opposite colors, they can form a color singlet subsystem or a closed string. When the parton number is large, there are many possibilities for two or more gluons to form CS states [6][7]. As is shown in Ref. [6], CC and CS states are not orthogonal to each other in perturbative sense. They belong to two different complete sets of color singlets in color space of the multipartonic state and are equivalent in the context of PQCD. However, they lead to different color connections on the hard-soft interface and may give rise to different hadronic states through the subsequent hadronization process [6][8]. Whether

the hadronization chooses CC or CS states as its starting point is determined by non-perturbative QCD dynamics. This question becomes critical in ultra-relativistic heavy ion collisions, since it is almost impossible to identify a unique color singlet chain in a bulk of partons.

The most efficient and practical way to study effects of CS connections on hadronic events is to modify the available event generators by substituting the CC connection with the CS one. Then we can use the new program to generate hadronic events and to investigate if there are any deviations from those generated with the default (CC) connection. An explicit example is given in Ref. [6], where a phenomenological CS model is proposed by incorporating CS connection into JETSET. The results show that there are no significant differences between CS and CC connections in terms of global properties of unbiased events [6]. This indicates that the available data for these properties does not rule out CS possibility. In other words, color connections beyond the traditional CC one, such as the CS connection discussed above, are also possible states on the interface between the hard and soft sectors in hadronic processes. To further confirm such an observation, it is natural to seek new observables in special events which may be sensitive to color connections. In this paper, we first give other properties of unbiased events except those in [6] and show these two different color connections can both describe data. Then we study some properties for three-jet events and compare them with the recent OPAL [13] and DELPHI data [14]. We find no evidence that CC is the unique color connection on the hard-soft interface. However, our investigation shows that the CC and CS states can lead to larger differences for some selected three-jet events where jets are well separated and the jet resolution scale, y_{cut} , is smaller. This could be put to further experimental test, e.g., by re-analysis of LEP data or in future Giga-Z experiment at linear collider.

The outline of this paper is as follows. In section 2 we give a brief description of the CS model [6]. We present in section 3 some results about unbiased events. In section 4 we study three-jet events and propose observables sensitive to color connections. A summary of results is given in section 5.

II. THE COLOR SEPARATE STATE MODEL

Our PQCD analysis shows that up to $O(1=N_c^2)$ a partonic system with $q\bar{q}$ and n gluons can be decomposed into two sub-singlets, one is the CC state made of $q\bar{q}$ and m gluons, the other is the CS state made of $(n-m)$ gluons [6]. The former forms an open string stretched between the quark and the anti-quark spanning m gluons, while the latter forms a closed string by the rest gluons. These CS states formed in the partonic system to $O(1=N_c^2)$ are called leading CS states. Based on this analysis a phenomenological model is constructed in the following way: (1) Only leading CS states are produced; (2) A CS state is produced with the relative weight given by the T-measure [15]. We implement the model into a Monte-Carlo program based on JETSET 7.4. In the program we just replace the default way of color connection at the end of parton cascade in JETSET 7.4, i.e. the CC connection, with the CS-allowed connection without touching all other parts. The CS cluster made of two or more gluons in a CS state hadronizes as closed strings [1].

Using this program, we have generated CS unbiased events and studied such global features as thrust, sphericity, oblateness and aplanarity. They are compared with those from CC unbiased events. The comparison shows that there are no significant differences between CS and CC unbiased events in terms of these global observables. In fact such a result is not surprising, because for unbiased events the global properties are mainly determined by PQCD parton cascade process and are not sensitive to hadronization details. This is nothing but the well-known property of local parton-hadron duality [16]. We therefore need to make further investigation in other observables more sensitive to color connections.

III. INVESTIGATION OF UNBIASED EVENTS

A. Identified hadron multiplicities and their momentum spectra

Two basic observables for hadronic events are multiplicities of identified hadrons and their momentum distributions. Using 6 million Monte Carlo events we calculate the average multiplicities and the inclusive momentum spectra for $\mu, K, p(p)$ in unbiased events. The statistical uncertainties for these observables are much less than those in data (about 1-2 order of magnitude lower than data). Our results for multiplicities together with data [17] at $\sqrt{s} = 10\text{ GeV}; 29\text{ GeV}$ and 91 GeV are listed in Table 1-3. The inclusive momentum spectra

for π , K , p (\bar{p}) at same energies are shown in Fig. 1a-c respectively. The data are taken from Ref. [17]. The results show that CS unbiased events agree with data at the same level as CC ones.

B. Ratio of baryon to meson and baryon-antibaryon correlation

It is well known that in e^+e^- annihilation most of the measured baryons are directly produced. Even if they are decay products of primary baryons, they keep more of their rapidities and momenta from their parents than most mesons do. Therefore, the spectra of the baryons in particular the correlation between baryon (B) and antibaryon (\bar{B}) could be a criteria to test different hadronization mechanism [18]. Here we investigate if this correlation can distinguish different color connections before hadronization.

In Lund string fragmentation model, baryon production is described by diquark or popcorn mechanism. The diquark production is controlled by the parameter $qq=q$, the ratio of the production rate of qq or $q\bar{q}$ to that of $q\bar{q}$ in color field [1]. The parameter $qq=q$ controls the ratio of baryon to meson. Six million Monte Carlo events are produced and the statistical uncertainty is much reduced as compared to data. The calculated ratios of baryon to meson at $\sqrt{s} = 10\text{ GeV}$, 29 GeV and 91 GeV are listed in Table 4. We see that there is no significant difference between CS and CC connections. For the CC connection, i.e. default setting in JETSET, one has to take different values of $qq=q$ at different energies to fit data ($qq=q = 0.06$ at $\sqrt{s} = 10\text{ GeV}$, and $qq=q = 0.1$ at other two energies). On the other hand, one can use an energy-independent value $qq=q = 0.1$ for CS events, and the results agree with data quite well.

The popcorn mechanism is realized by the popcorn parameter:

$$= \frac{P(BM\bar{B})}{P(B\bar{B}) + P(BM\bar{B})}; \quad (1)$$

where $= 1$ means that a meson is always produced between B and \bar{B} , while in the other limit $= 0$ it is not at all. The popcorn parameter also describes the $B\bar{B}$ correlation. Here we take $= 0.5$ and calculated the pp , and $p = \bar{p}$ rapidity correlations for unbiased events at Z^0 pole. The results are shown in Fig. 2a-c. Both CS and CC connections agree with data [19] at the same level.

Besides the global properties studied in [6], we have investigated other properties for

unbiased events with CS or CC color connections. The results obtained in both cases are consistent with data. For some results the agreement is even better in CS events.

IV. INVESTIGATION OF THREE-JET EVENTS AT Z^0 POLE

Since different color connections lead to different color strings and may cover different phase space, one expects that the CS state should have some effects on the energy and momentum flow of final hadrons. So the impact of the CS connection could be observable in some specific events. Currently a large number of three-jet events, where a gluon-jet can be identified, are available at Z^0 resonance energy at LEP I. It is highly possible that the gluon-jet could be the fragmentation product of gluonic color singlet clusters which are CS singlets. Therefore, we expect that some sensitive observables should be out there in a specified window of phase space around the gluon jet. In the following, we will study the properties of three-jet events at Z^0 resonance energy to probe the possible effect of CS states. We note that a similar work has been done for two-jet events [20].

A. Selection of three-jet events

We use Durham jet algorithm [21] to select three-jet events. In the algorithm, particles are grouped into jets based on a cut-off variable y_{cut} defined as follows. For each pair of particles i and j with energies E_i and E_j respectively and their opening angle θ_{ij} , one defines y_{ij} as

$$y_{ij} = \frac{2 \min(E_i^2, E_j^2) (1 - \cos \theta_{ij})}{E_{\text{vis}}^2}; \quad (2)$$

where E_{vis} is the total visible energy in the event. Given a cut-off value y_{cut} , one can put all particles into one jet where all y_{ij} 's for any two particles inside the jet are smaller than y_{cut} , while $y_{ij} > y_{\text{cut}}$ for the case with one inside the jet and the other outside it. The number of particles in a jet is then the multiplicity of the jet. Increasing y_{cut} makes the fraction of multi-jet events lower because y_{cut} is actually a jet resolution parameter.

We have calculated the fraction of three-jet events as function of y_{cut} . Both color connections agree with data [22]. We have also calculated the charged particle multiplicity for three-jet events at some values of y_{cut} and compared our results with data [23]. There is no sizable difference between CS and CC events.

B. Particle multiplicities and momentum spectra of identified hadrons in Y events

Recently OPAL collaboration has measured the charged particle multiplicity N_{ch} for three-jet light-quark events of the so-called Y shape from Z^0 decay as function of the angle between the two jets with lowest energies [13]. The jets are defined by Durham jet-order. The resolution y_{cut} is adjusted separately for each tagged uds event so that three jets can be exactly reconstructed. They applied this procedure instead of using a fixed resolution value just to avoid introducing a bias into the gluon jet. The jets are labelled 1,2 and 3 in such an order that jet 1 carries the highest energy. Only those events, the so-called Y events, are kept where the angles between the most energetic jet and the rest two are the same up to 3°. We are particularly interested in these data which could be used to test our CS model. We choose such Y events from 10 million Monte Carlo samples at Z^0 pole accommodating the same experimental condition. The calculated particle multiplicities varied with angle are shown in Fig. 3. One can see that there is some difference between two types of color connections and that results from the CC connection seem to agree with data better than those from the CS one. However, such a difference is not significant enough to discriminate the two in terms of data. The multiplicity distribution calculated for these Y events with $0 < \theta < 120^\circ$ is shown in Fig. 4. Besides these results, we also calculated other observables measured in Ref. [13]. All these results fail to show any significant difference between the two types of connections.

DELPHI collaboration has measured momentum spectra of identified hadrons in quark jets of all species (dusdb) together with gluon jets for Y events [14]. The three-jet events are identified by Durham algorithm with $y_{cut} = 0.015$. The jets are also labelled in descending order of jet energies. The Y events are obtained with $\theta_{23} > 2^\circ$ [150° - 15°; 150° + 15°], where θ_2 and θ_3 are angles between the highest energetic jet and other two jets with lower energies. In order to compare with data of this experiment, we calculate the momentum spectra of identified hadrons in quark and gluon jets for Y events with the same constraints as in the experiment. The samples are 10 million Monte Carlo events at Z^0 pole. The results are shown in Fig. 5. One sees that it is hard to distinguish the CS from the CC connection by comparison with data. So up to now, no evidence has ruled out the CS connection as a possible candidate state on the hard-soft interface.

However, the above results imply that some differences between the CC and CS connec-

tions are present. In the next section we will investigate whether they could be amplified by choosing suitable y_{cut} and the angles between jets.

C. Observables in special three-jet events

One expects that more sensitive observables come from the phase space around the gluon jet. A normal method to identify the gluon-jet in experiments is to label three jets by their energies in descending order $E_1 > E_2 > E_3$. The most energetic jet (jet 1) is usually recognised as the quark-jet (or antiquark-jet), and the one with the smallest energy (jet 3) as the gluon jet. We denote the angle between the first and the second jet by θ_{12} and that between the first and the third one by θ_{13} .

We look at three-jet events with restricted range of θ_{12} and θ_{13} . We calculate charged particle multiplicities whose sensitivity to different color connections varies with θ_{12} and θ_{13} . We find that only those events where jet 3 is well separated from jet 1 and 2 exhibit considerable difference in multiplicity from color connections. Considering both the statistics and the sensitivity to color connection, we choose $100 < \theta_{12}; \theta_{13} < 160^\circ$. We also find that the difference increases with decreasing y_{cut} . Here we use a fixed value of the resolution parameter y_{cut} instead of one for each three-jet event.

Now we focus on the gluon jet in three-jet events. We calculate the multiplicity, the invariant mass and the longitudinal momentum of the gluon jet as functions of y_{cut} . Compared with those from CC connections, the results from CS ones are found to be smaller for the multiplicity and the invariant mass, and larger for the longitudinal momentum. We also find that the difference between CC and CS is more significant for smaller y_{cut} , as shown in Fig.6. We select three-jet events from 10 million Monte Carlo samples at Z^0 pole. Our numerical results are given with constraint $100 < \theta_{12}; \theta_{13} < 160^\circ$ at $y_{\text{cut}} = 0.0005$. The fraction of selected three-jet events in the total ones is about 0.502%. We give in Fig. 7 the multiplicity distribution. The result shows that two different ways of color connections do bring larger differences in the final hadronic state. The shapes of two multiplicity distributions look similar, but the peak of the distribution for the CS case locates at a smaller value of n_{ch} than that for the CC case, implying a lower average multiplicity: $\langle n_{\text{ch}} \rangle_{\text{CS}} = 18.22$, $\langle n_{\text{ch}} \rangle_{\text{CC}} = 19.41$, and the difference is $4 \langle n_{\text{ch}} \rangle = 1.19$. The reason is obvious: in CS events several groups of gluons form color singlet clusters and each hadronizes independently, which

makes the effective energy to produce hadrons smaller than that in CC events.

Considering that the average longitudinal momentum of the gluon-jet for CS events is larger than that for CC ones, we define the following observable:

$$T = \frac{\sum_i^P p_{zi}}{\sum_i^J p_{iJ}}; \quad (3)$$

where p_i and p_{zi} are the 3-momentum and its longitudinal component of a final state hadron in the gluon-jet respectively. Here longitudinal means parallel to the gluon-jet axis. The observable T is introduced to amplify the difference of CC and CS events. The distribution of observable T with both CS and CC connections is given in Fig. (8a) and shows that T is a sensitive observable to color connections. We also calculated the spectra of the charged particle multiplicity, the rapidity and the invariant mass in the gluon-jet, as shown in Fig.(8b-d). One sees that now the predicted distinction between CC and CS connections is obvious. The reason is that the formation of closed strings in a gluon jet with the CS connection takes more momentum along the the direction of the mother parton, i.e. the gluon, than the CC one, which makes the gluon-jet thinner. This point can be further strengthened by the spectra of the polar angle and the longitudinal momentum for hadrons in the gluon jet. We note that all results in Fig.8 are consistent with each other.

V. SUMMARY

In this paper, the comparison of our results with the available data up to now shows that the CS state is a possible choice for the hard-soft interface in hadronic processes. This is consistent with PQCD analysis. Such a picture of colour connection is natural for a deconfined quark-gluon system, where a huge number of partons interact with each other and it is impossible to identify a unique color singlet chain. This paper is also an attempt for searching observables in special events where the differences between the CS and CC states are significant. The identification of these differences in experiments will deepen our understanding of the hard-soft interface in hadronic processes.

By a careful look at certain type of three-jet events with smaller y_{cut} , where angles between jets are restricted in a specific range, we have found more sensitive observables to color connections. The difference between CC and CS connections is amplified in the charged particle multiplicity and properties of the gluon-jet in these events. The distinction

between CS and CC events can be put to test by re-analysing the LET-I data and/or in future experiments such as Giga-Z at linear collider.

Acknowledgements

The authors thank Z.-T. Liang and Z.-G. Si for insightful discussions. This work is supported in part by the National Natural Science Foundation of China under grant No. 10075031 and 10205009.

-
- [1] B. Andersson, G. Gustafson, G. Ingelman and T. Sjöstrand, *Phys. Rep.* 97, 31 (1983).
 - [2] B. R. Webber, *Nucl. Phys. B* 238, 492 (1984); G. Marchesini and B. R. Webber, *Nucl. Phys. B* 238, 1 (1984).
 - [3] T. Sjöstrand, *Comp. Phys. Commun.* 82, 74 (1994).
 - [4] G. Marchesini et al., *Comp. Phys. Commun.* 67, 465 (1992); G. Corcella et al., *JHEP* 0101, 010 (2001).
 - [5] C. Friberg, G. Gustafson, and J. Hakkinen, *Nucl. Phys. B* 490, 289 (1997).
 - [6] Q. Wang, G. Gustafson, and Q.-B. Xie, *Phys. Rev. D* 62, 054004 (2000).
 - [7] Q. Wang, Q.-B. Xie, *Phys. Rev. D* 52, 1469 (1995); Q. Wang, Q.-B. Xie, and Z.-G. Si, *Phys. Lett. B* 388, 346 (1996).
 - [8] Q. Wang, G. Gustafson, Y. Jin, and Q.-B. Xie, *Phys. Rev. D* 64, 012006 (2001).
 - [9] F. Maltoni, K. Paul, T. Stelzer, and S. Willenbrock, *Phys. Rev. D* 67, 014026 (2003).
 - [10] Y. Jin, Q.-B. Xie, and S.-Y. Li, *High Energy Phys. & Nucl. Phys.* 27, 282 (2003) (in Chinese).
 - [11] T. Sjöstrand, and V. A. Khoze, *Z. Phys. C* 62, 291 (1994); *Phys. Rev. Lett.* 72, 28 (1994).
 - [12] L. Lonnblad, *Z. Phys. C* 70, 107 (1996).
 - [13] OPAL Collab., G. Abbiendi et al., *Eur. Phys. J. C* 23, 597 (2002).
 - [14] DELPHI Collab., P. Abreu et al., *Eur. Phys. J. C* 17, 207 (2000).
 - [15] B. Andersson, and G. Gustafson, and B. Soderberg, *Nucl. Phys. B* 264, 29 (1986).
 - [16] B. Andersson, P. Dahlgvist, and G. Gustafson, *Z. Phys. C* 44, 461 (1989); 44, 455 (1989); Y. I. Azimov, Y. L. Dokshitzer, V. A. Khoze, and S. I. Troyan, *Z. Phys. C* 27, 65 (1985).
 - [17] Particle Data Group, D. E. Groom et al., *Eur. Phys. J. C* 15, 1 (2000) and references therein.

- [18] Z.-G. Si, Q.-B. Xie, and Q. Wang, Commun. Theor. Phys. 28, 85 (1997).
- [19] DELPHI Collab., P. Abreu et al, Phys. Lett. B 416, 247 (1998).
- [20] S.-Y. Li, F.-L. Shao, Q.-B. Xie, and Q. Wang, Phys. Rev. D 65, 077503 (2002).
- [21] S. Catani et al, Phys. Lett. B 269, 432 (1991); W. J. Stirling, J. Phys. G 17, 1567 (1991).
- [22] OPAL Collab., P. D. Acton et al, Z. Phys. C 55, 1 (1992).
- [23] DELPHI Collab., P. Abreu et al, Z. Phys. C 56, 63 (1992).

TABLE I: Average multiplicities for hadrons in e^+e^- annihilation at $\sqrt{s} = 10\text{ GeV}$. For each entry, the charge conjugate state is also included if it is different from the entry itself.

particle	data		CC	CS
π^+	6.6	0.2	6.12	6.31
π^0	3.2	0.3	3.59	3.71
	0.2	0.04	0.34	0.37
$(770)^0$	0.35	0.04	0.50	0.53
η	0.30	0.08	0.41	0.44
η'	0.03	0.01	0.095	0.099
(1020)	0.044	0.003	0.073	0.085
K^+	0.90	0.04	0.98	0.99
K^0	0.91	0.05	0.85	0.85
$K(892)^+$	0.27	0.03	0.42	0.41
$K(892)^0$	0.29	0.03	0.37	0.36
D^+	0.16	0.03	0.17	0.17
D^0	0.37	0.06	0.48	0.48
$D(2012)^+$	0.22	0.04	0.24	0.24
D_s^+	0.13	0.02	0.097	0.097
p	0.253	0.016	0.342	0.298
$(1232)^{++}$	0.040	0.010	0.051	0.041
	0.080	0.007	0.107	0.093
Λ^0	0.023	0.008	0.021	0.019
	0.0059	0.0007	0.0074	0.0065
(1385)	0.010	0.0020	0.0172	0.0136
$(1530)^0$	0.0015	0.0006	0.0013	0.0011
Λ_c^+	0.100	0.030	0.049	0.044

TABLE II: Same as Table 1 except at $\sqrt{s} = 29\text{ GeV}$

particle	data		CC	CS
π^+	10.3	0.4	10.6	11.0
π^0	5.83	0.28	6.11	6.32
	0.61	0.07	0.61	0.66
$(770)^0$	0.81	0.08	0.91	0.96
η			0.79	0.83
η'	0.26	0.10	0.18	0.18
(1020)	0.085	0.011	0.117	0.132
K^+	1.48	0.09	1.52	1.54
K^0	1.48	0.07	1.34	1.35
$K(892)^+$	0.64	0.05	0.69	0.68
D^+	0.17	0.03	0.19	0.19
D^0	0.45	0.07	0.55	0.55
$D(2012)^+$	0.43	0.07	0.27	0.27
D_s^+	0.45	0.20	0.12	0.12
p	0.640	0.050	0.694	0.631
$(1232)^{++}$			0.109	0.094
	0.205	0.010	0.214	0.193
ρ^0	0.023	0.008	0.021	0.019
	0.0176	0.0027	0.0150	0.0133
(1385)	0.033	0.008	0.038	0.032
$(1530)^0$			0.0027	0.0022
χ_c^+	0.110	0.050	0.068	0.067

TABLE III: Same as Table 1 except at $\bar{s} = 91\text{G eV}$

particle	data		CC	CS
$+$	16.99	0.27	16.94	17.06
0	9.47	0.54	9.58	9.69
	0.971	0.030	1.003	1.043
$(770)^0$	1.231	0.098	1.503	1.522
$!$	1.08	0.12	1.35	1.36
0	0.156	0.021	0.297	0.295
(1020)	0.0963	0.0032	0.1932	0.2077
K^+	2.242	0.063	2.300	2.305
K^0	2.013	0.033	2.070	2.058
$K(892)^+$	0.715	0.059	1.102	1.074
$K(892)^0$	0.738	0.024	1.096	1.069
D^+	0.175	0.016	0.175	0.174
D^0	0.454	0.030	0.489	0.489
$D(2012)^+$	0.183	0.010	0.240	0.270
D_s^+	0.131	0.21	0.130	0.130
p	1.048	0.045	1.195	1.090
$(1232)^{++}$	0.085	0.014	0.188	0.164
	0.374	0.009	0.385	0.351
0	0.070	0.012	0.073	0.067
	0.174	0.009	0.140	0.127
	0.0258	0.0010	0.0274	0.0248
(1385)	0.0462	0.0028	0.0738	0.0652
$(1530)^0$	0.0055	0.0005	0.0054	0.0048
$_c^+$	0.078	0.017	0.059	0.059

TABLE IV : The ratios of baryon to meson. We set $q\bar{q}=q=0.1$. The data are from Ref. [17]. The numbers marked with "*" are those beyond two standard deviations from data.

\sqrt{s} [GeV]	particle	data	CC	CS	
91	p= *	0.062	0.003	0.071	0.064
	p=K *	0.467	0.024	0.520	0.473
	=K *	0.167	0.006	0.167	0.152
	(1385) =K *	0.0646	0.0066	0.0670	0.0607
	(1530) ⁰ =K *	0.0075	0.0007	0.0049	0.0045
29	p= *	0.062	0.005	0.065	0.057
	p=K *	0.432	0.043	0.453	0.407
	=K *	0.139	0.011	0.141	0.126
	(1385) =K *	0.0516	0.0131	0.0553	0.0468
	(1530) ⁰ =K *			0.0045	0.0038
10	p= *	0.038	0.003	0.056	0.047
	p=K *	0.281	0.022	0.349	0.301
	=K *	0.089	0.009	0.109	0.094
	(1385) =K *	0.0393	0.0086	0.0410	0.0332
	(1530) ⁰ =K *	0.0052	0.0021	0.0035	0.0031

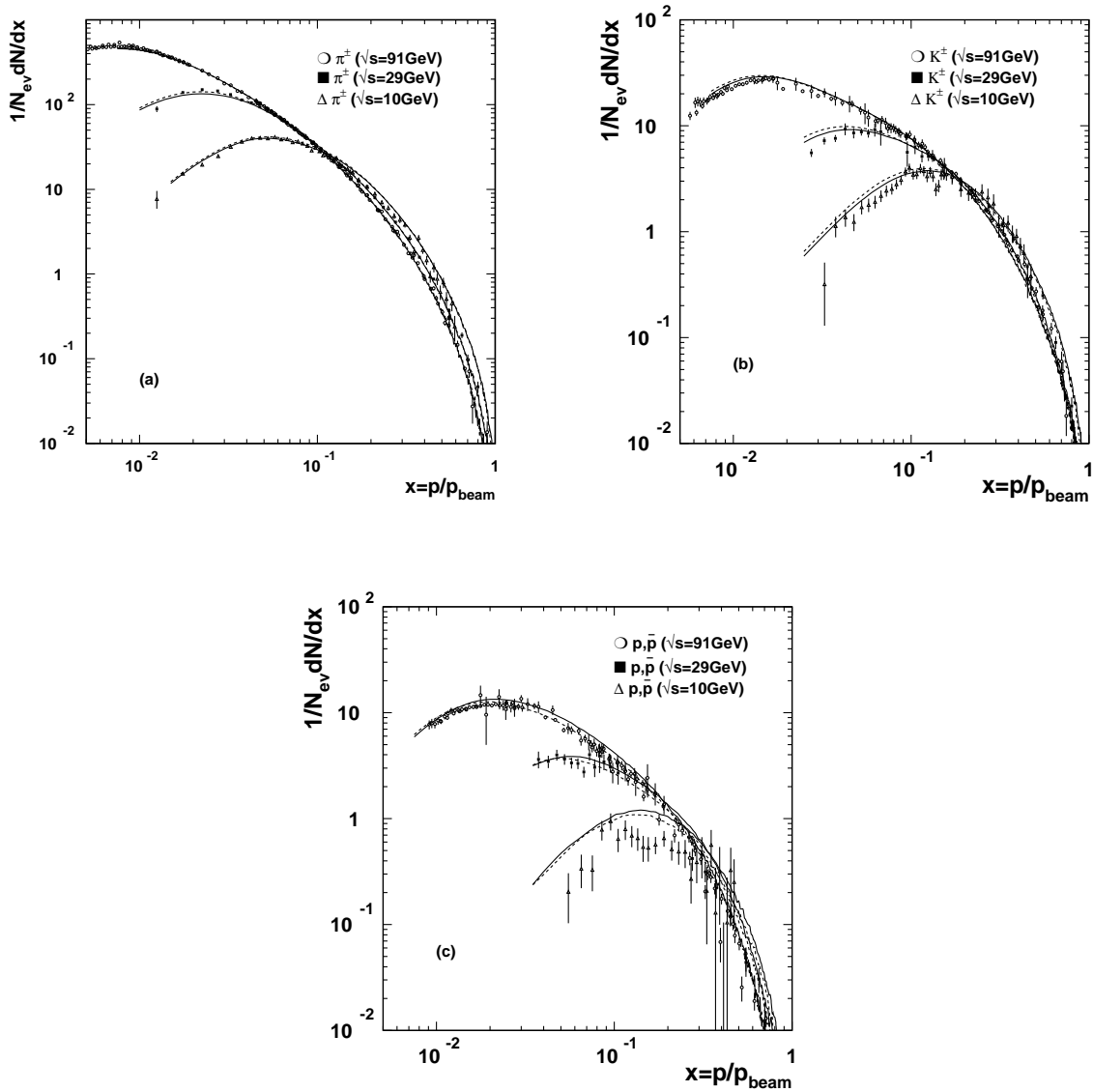


FIG. 1: Inclusive cross sections ($1/N_{ev} dN/dx$) for (a) π^\pm , (b) K^\pm and (c) p, \bar{p} as function of $x = p/p_{beam}$. The solid lines are from CC events and the dashed ones from CS events. The data are taken from Ref. [17].

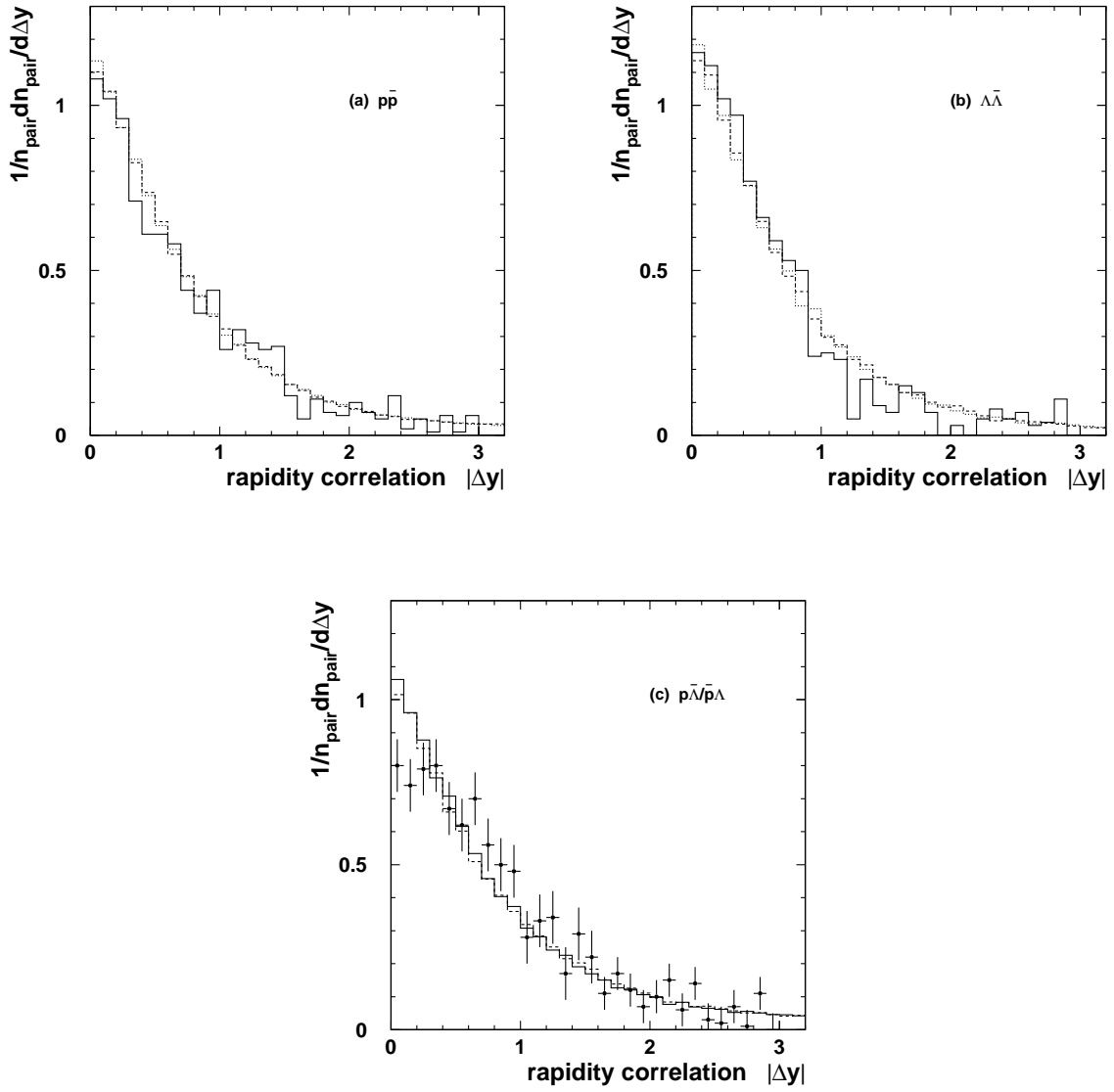


FIG. 2: Rapidity differences of B B pairs with respect to the thrust axis of the event. In (a) and (b), the solid histograms are data from Ref. [19]; The dashed and dotted lines are from CC and CS events respectively; In (c), the solid and dashed lines are from CC and CS events respectively; The black squares with error bars are data [19].

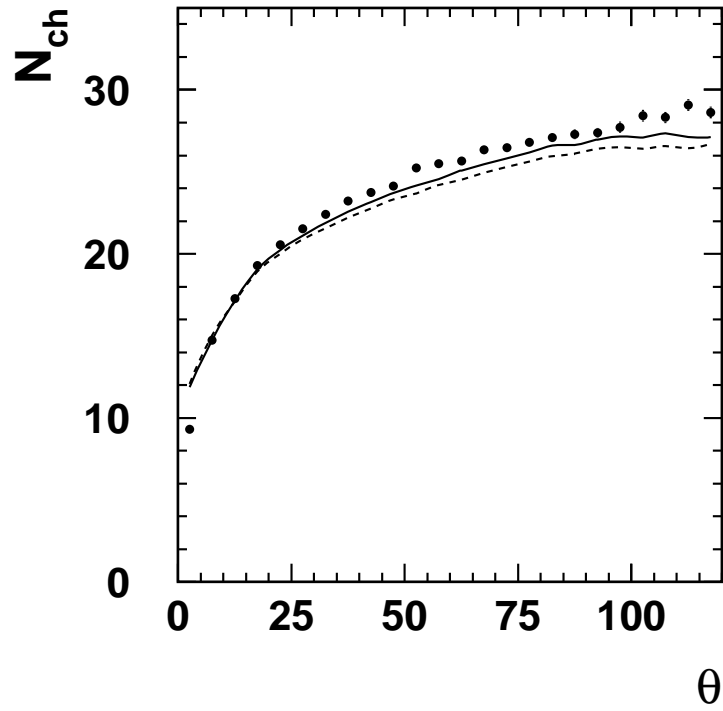


FIG . 3: The particle multiplicity n_{ch} for Y events as function of the angle θ between two jets of the lowest energies. The solid line is from CC events and the dashed one from CS events; The data are taken from Ref. [13].

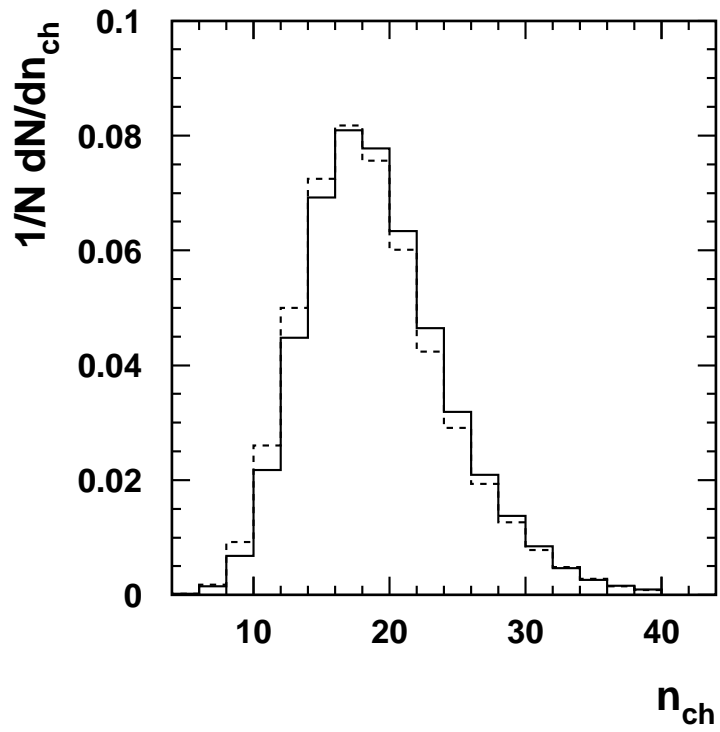


FIG . 4: Multiplicity distribution of charged particles in three-jet light-quark Y events. The range of angle is $[0 ; 120]$. The solid line is from CC events and the dashed line is from CS ones.

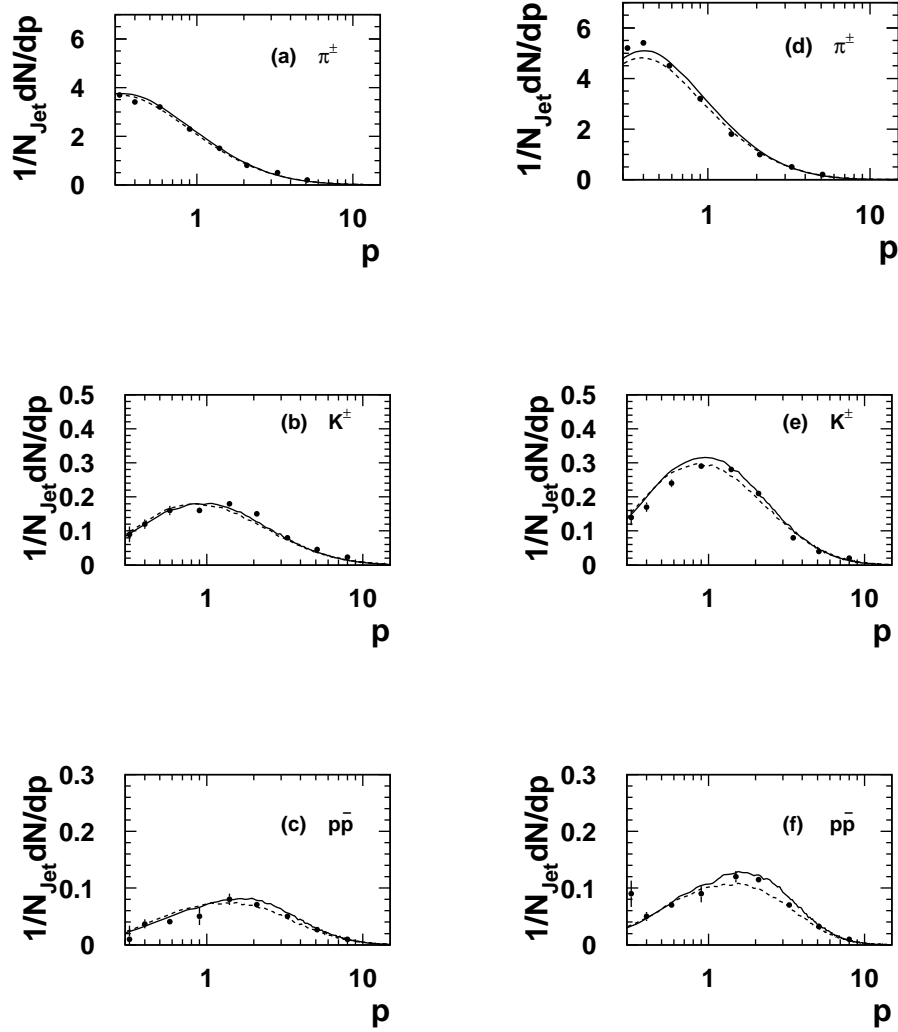


FIG. 5: Momentum spectra of identified hadrons in quark and gluon jets for Y events. Figure (a) is spectra of pions, (b) kaons, and (c) protons in quark jets. (d), (e) and (f) are corresponding spectra in gluon jets. The solid line is from CC events and the dashed one is from CS events. The data are taken from Ref. [14].

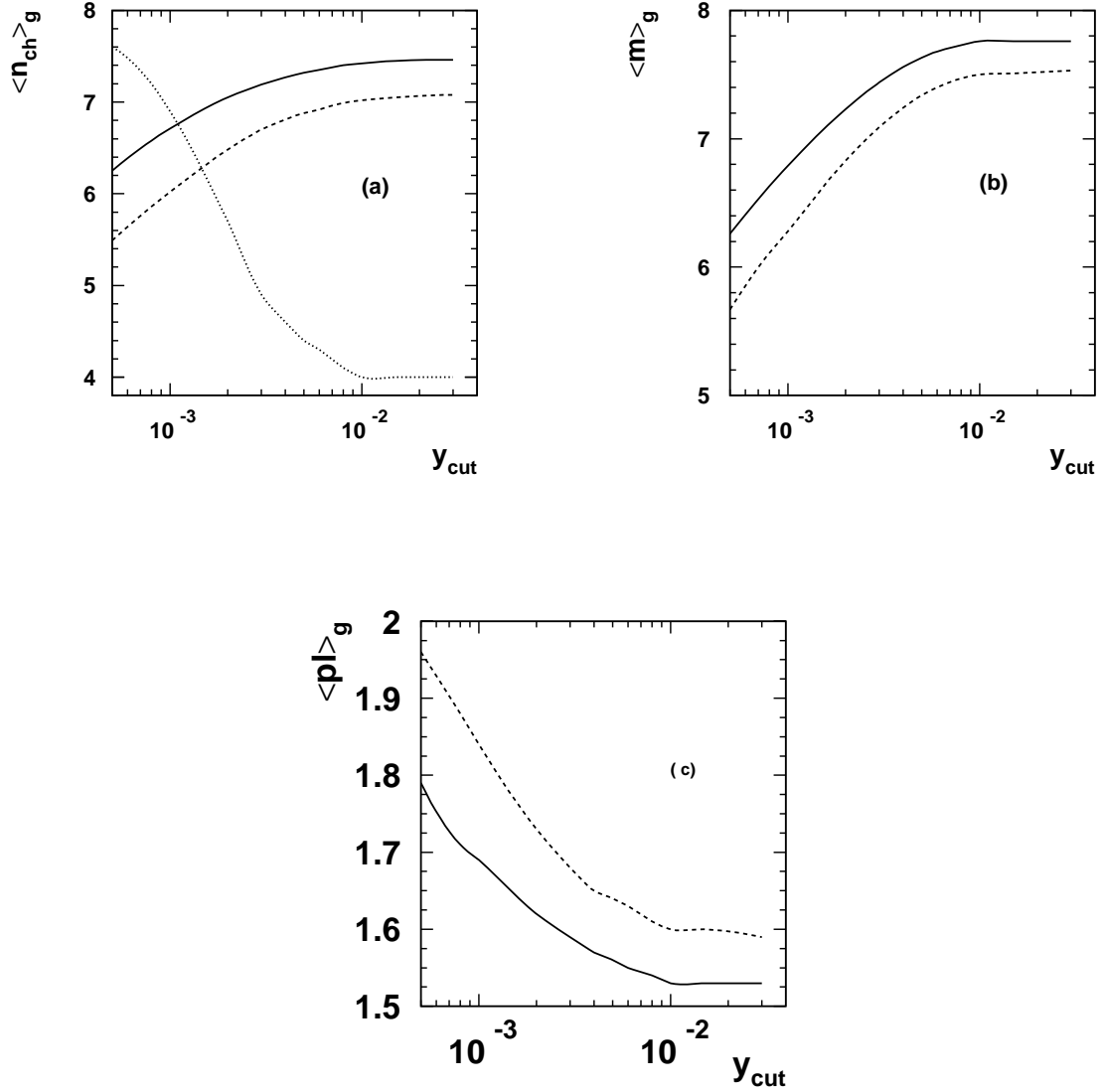


FIG. 6: The average values of observables for the gluon-jet in three-jet events as functions y_{cut} at Z^0 pole. n_{12} and n_{13} are limited within $[100; 160]$. (a) Multiplicity. The solid, dashed and dotted lines are for CC, CS and their difference ($n_{12} - n_{13}$) respectively; (b) Invariant mass; (c) Average longitudinal momentum. For both (b) and (c), the solid and dashed lines are for CC and CS events respectively.

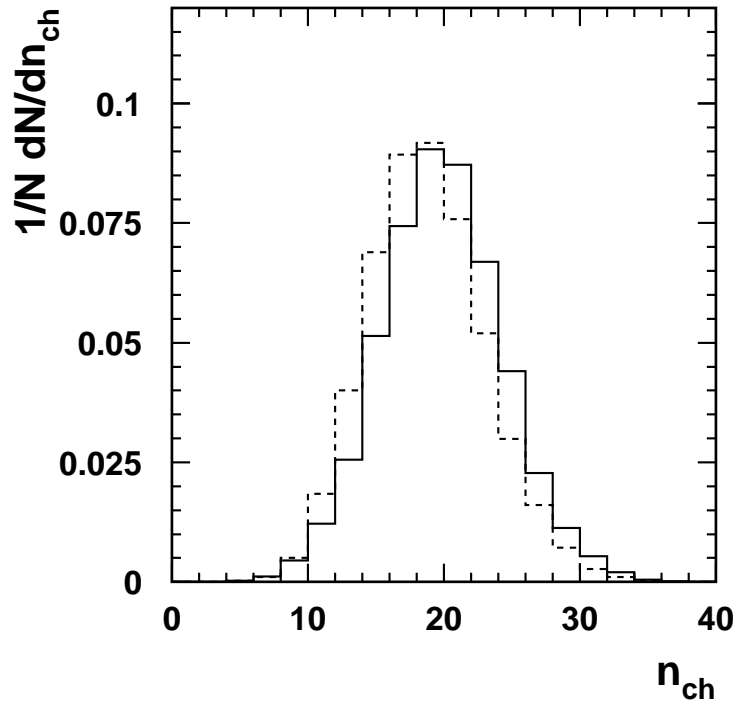


FIG . 7: The multiplicity distribution of charged particles in the selected three-jet events ($v_{cut} = 0.0005$). n_{12} and n_{13} are limited within $[100 ; 160]$. The solid and dotted lines are for the CC and CS events respectively.

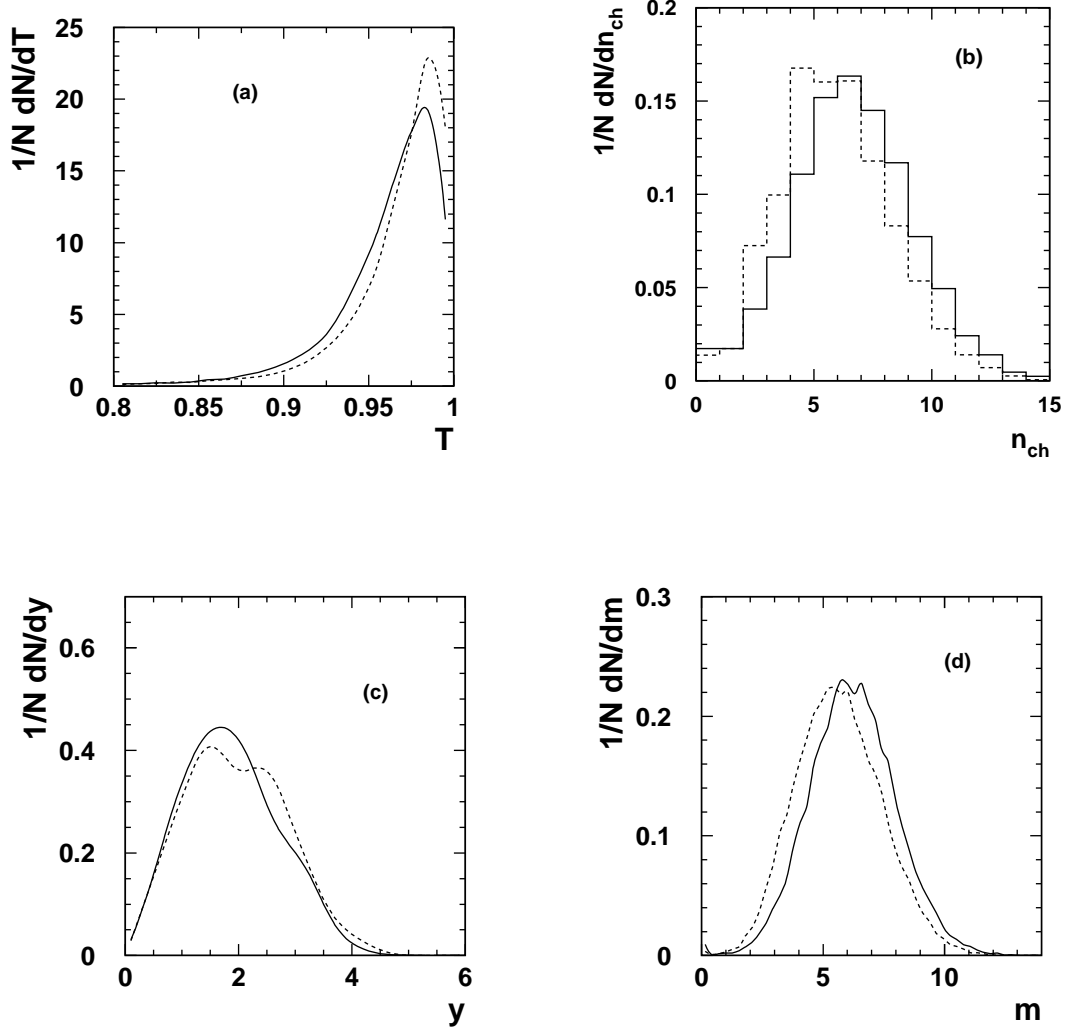


FIG. 8: Distributions of observables for the gluon jet in three-jet events ($y_{cut} = 0.0005$). n_{12} and n_{13} are limited within $[100; 160]$. (a) T distribution; (b) The distribution of the charged particle multiplicity; (c) The rapidity distribution; (d) The invariant mass distribution. The solid lines are for CC events, and the dashed lines are for CS events.